

# Interactive interpretation of 3D surfaces in field-based geosciences using mobile devices - concepts, challenges and applications

Melanie Kröhnert<sup>a,\*</sup>, Christian Kehl<sup>e</sup>, Sophie Viseur<sup>b</sup>, Simon J. Buckley<sup>c,d</sup>

<sup>a</sup>*Institute for Photogrammetry & Remote Sensing, TU Dresden, Helmholtzstr. 10, 01069 Dresden, Germany*

<sup>b</sup>*Aix Marseille Université, CNRS, IRD, CEREGE UM 34, Dept. Sedimentary and Reservoir Systems, 13001 Marseille, France*

<sup>c</sup>*Uni Research AS – CIPR, Nygårdsgaten 112, 5008 Bergen, Norway*

<sup>d</sup>*Department of Earth Science, University of Bergen, Allégaten 41, 5007 Bergen, Norway*

<sup>e</sup>*Danmarks Tekniske Universitet, DTU Compute, Richard Petersens Plads, Building 321/208, 2800 Kongens Lyngby, Denmark*

---

## Abstract

**Keywords:** discrete geometry, surface reconstruction, volume reconstruction, surface parameterization, digital outcrops

**2010 MSC:** 00-01, 99-00

---

## 1. Introduction

A considerable number of domains within the geosciences rely on digitised natural observations and their interpretation to steer and constrain numerical models. Published (semi-)automatic interpretation methods emerged within the  
5 past decade that support the digital documentation of observations and interpretations. These advanced interpretation techniques require increasingly complex computing that is restricted to office-based work environments, which poses a problem for field-based studies. Domains such as hydrology, geology or glaciology hence established multi-stage procedures where observations are taken  
10 manually in the field and later digitised in the office. This is disadvantageous

---

\*Corresponding author

*Email addresses:* melanie.kroehnert@tu-dresden.de (Melanie Kröhnert), chke@dtu.dk (Christian Kehl), viseur@cerege.fr (Sophie Viseur), Simon.Buckley@uni.no (Simon J. Buckley)

and within the referred domains, there is an increasing desire to facilitate digital interpretations in the field at the study location. Mobile computing equipment (e.g. smartphones and tablets) are one technological option to facilitate such digital field-based workflows. These devices are nowadays ubiquitous and can easily be equipped in field-based research. Also, as seen in technical magazines and the general media, the range of available devices continuously increases, which allows to find a "fit-for-purpose" device to each specific situation. New application cases, which are demonstrated and discussed in this article, and commitment within geoscience- and computer technology industry lead to an increasing interest in this cross-disciplinary domain between mobile computing and geoscientific interpretation.

Next to easily available, pocket-format computing devices, the required three-dimensional base data for modern applications also need to be available and being processed in a "mobile-ready" manner. The availability of topographic 3D surface data is steadily increasing due to easy-to-use software and instrumentation for surface generation (e.g. drones, structure from motion (SfM) [?] and multi-view geometry [?], satellite digital elevation models (DEMs)). Furthermore, crowdsourced data and Volunteered Geographic Information (VGI) contribute to the geoscience data inventory, which is acquired by citizen scientists.

Domain-specific mobile software is required in order allow for data interaction on the available mobile devices. Specific challenges such as power consumption, multi-manufacturer support, smart sensor utilisation and device intercommunication distinguish mobile software from common desktop software. This leads to a very different design electronics design of tablets and smartphones in comparison to desktop PCs and laptops, which in turn means that existing approaches for digital data processing and interpretation are not transferable as-is to this new computing domain. Even when considering the fast technological development, there are some challenges within mobile device software development that are rooted in the technology itself: user interfaces need to be specifically designed for mobile devices so to utilise touch screen interfaces, nat-

ural language interfaces and gesture interaction (e.g. "swipe" and "optical lens" motions). global navigation satellite system (GNSS)-based geo-localisation accuracy, as delivered by the integrated-circuit sensor of mobile, is inferior to  
45 common user expectations and requirements in geoscientific studies. The modalities of sensor data delivery (be it hardware sensor or software emulation), photo capturing and processing, and the computational capabilities of mobile devices differ significantly between each vendors. Short-comings such as inappropriate data structuring, visual object correlation and registration, increasing  
50 data volumes and the unavailability of off-the-shelf program codes further complicate the technological development. Addressing the demonstrated challenges distinguishes the mobile application development and common desktop software development for geoscience purposes. **the same as in line 34?**

This article demonstrates how the above-listed challenges can be addressed  
55 to provide, in the end, the desired added value for field-based research. This demonstration addresses the 3D data annotation and interpretation for two use cases within the domains of surface hydrology and (petroleum) geology. The content covered in the article is a detail-driven extension of earlier published research [1], focussing on extensive measurements to verify the reasoning and  
60 statements of previous studies.

The sections within this article adhere to the following structure: First, the use cases are presented as opening statements to introduce field-related tasks that are to be addressed with mobile device technology. Secondly, different 3D surface data representations are introduced that employed within this technical  
65 research. Thirdly, algorithmic baseline concepts that are key for interpreting 3D data on mobile devices are introduced, summarising project-internal development by the authors as well as referencing key literature on the subject. Fourth, the algorithms are mapped to the specific mobile technologies and components. The technologies and major parameters that impact the target use case applica-  
70 tion are highlighted. Finally, we showcase and discuss how available mobile systems are used in application scenarios from hydrology and petroleum geology to improve data analysis and integrate outdoor measurements in digital

workflows. Then, the article is finalized with some concluding remarks and a discussion for future developments in this research trajectory.

## 75 2. Target case studies

TO-BE-FILLED

## 3. Representation basis – Geometry and Radiometry

iiiiiii HEAD Various representation forms for 3D terrain data are available. While early digital systems used gridded DEMs for their simplicity and compact  
80 storage [2, 3], digital surface models (DSMs) and triangulated irregular networks (TINs) are dominating most terrain-based systems for application-specific analysis [4, 5]. A useful example can be seen in [6] for glaciology, where the authors use a triangulated digital surface model to represent a Patagonian glacier front. For triangular surfaces, it is important to distinguish geometrically valid TINs  
85 from polygon soup surfaces. While the latter is often employed in early stages of mesh-based software systems due to its simplicity and ease of implementation, valid TINs are employed in mature stages of the analysis. This is because some automated analysis (e.g. auto-interpretation, volume derivation) require clean surfaces with coherently outward-oriented surface normals.

90 In geoscience domains such as petroleum geology, texture- and color information are vital for interpretation- and analysis tasks. In these cases, as demonstrated by Buckley et. al [4] and Caumon et. al [5], the TIN is supplemented with photographic information that is projected on the surface as textures.

[ASK SIMON FOR USAGE OF IMAGES FROM VOG - use own reconstruction of Whitby cliffs for nice TINs]  
95

In other geoscience domains, such as hydrology and free surface flow management, on the one hand georeferenced laser scanner point clouds, and on the other one colored point data streams provided by terrestrial photogrammetry for small- or unmanned aerial vehicle (UAV) for large-scale use cases, both processed by application of SfM, are used for several tasks like coastal monitoring  
100

[7, 8], soil erosion and rain-induced landslide observation or even monitoring river’s topography [9]. Nevertheless, new approaches for low-cost and on-the-fly river monitoring [10] and simulation [11] arise due to globally increasing flash flood events after heavy rainfalls [12] that are further addressed in section. Since  
105 SfM became state of the art in geosciences, the acquisition of (true-)colored ”point cloud“ models is not that difficult and commonly employed because of their rapid processing (compared to conventional approaches like terrestrial laser scanning (TLS)). Regarding 3D annotation, nearest neighbour analysis provide an opportunity whereby surface triangulation can be avoided.

110 The stated base concepts of geometric representation and radiometric texture information are also valid for mobile device software. Because of the limited processing speed of mobile chipsets, the usage of point cloud appears most common within the graphics literature (e.g. Garcia et. al [13]). Because the sparse vertex distribution in point clouds causes problems in the data analysis, DEMs  
115 have seen a revival in the mobile computing domain. DEMs provide dense, closed geometric models that can be rendered and processed very efficiently. Furthermore, with the inferior memory capacity of mobile devices in comparison to laptops and workstations, the possible compression options for point clouds and DEMs are advantageous. Base mapping applications such as Google  
120 Maps use DEMs, derived from light detection and range (lidar) or satellite data [14], as their main topographic data representation. Other systems within the geosciences processing 3D data on mobile devices, such as ”Outcrop“ and Geological Registration and Interpretation Toolset (GRIT), employ genuine textured triangulated DSM from lidar, drone or SfM sources.

125 The chosen form of model representation significantly impacts the algorithms and analytical capabilities employed on the mobile device. Although all algorithms presented in this article work on either form of representation, some of the algorithms favour the treatment of triangulated surfaces (e.g. image-to-geometry registration, guided interpretation), while others clearly favour point-  
130 based representations (e.g. rendering).

## 4. Algorithms

This section demonstrates novel- as well as existing algorithms and methods on mobile devices that are used for solving analysis tasks in the geoscience use cases laid out in section ?? . As mentioned before, the effectiveness of each  
135 algorithm depends on the applied model representation.

### 4.1. Image-to-geometry registration

- short description what it does
- how is it generally employed
- relation to mobile devices
- 140 • approaches and implementation known on mobile devices
- integration to the above-mentioned use cases

Image-to-geometry algorithms aim at registering a 2D image to a given 3D surface, providing a transformation from 2D coordinate system to 3D coordinate system as follows:

$$P' = \begin{pmatrix} u \\ v \\ w \end{pmatrix} = [R_{3,3}|T_{1,3}] \cdot P \quad (1)$$

$$P = \begin{pmatrix} x \\ y \\ z \end{pmatrix} \quad (2)$$

$$P' \in \mathbb{R}^2 = \frac{P'}{w} \quad (3)$$

145 Using this coordinate system transformation on combination with a known interior camera orientation, it is possible to projectively map entire images on the surface just as surface texturing does. It is also possible to map specific objects on the image, such as image-based interpretations, on the surface. In

the geosciences, these algorithms are employed to create a direct correlation  
150 between 3D model and the screen- or image space on which annotations and  
interpretations are based on [15].

- feature-based registration: detect prominent points or edges in the input  
2D images and a rendered representation of the 3D model
- different concept for registration:
  - 155 – for mesh models, 2D feature locations are raycasted using camera  
projection and the 3D model in background; 3D feature location  
determined upon ray-plane intersection
  - for point-based models, raycasting doesn't directly work as point  
cannot be intersected; prominent solution is employing a smart ren-  
160 dering technique that expands the point into an area, and generate  
a depth map; after depth map generation, the 3D coordinate of a 2D  
feature map can be read directly from the depth map; drawback of  
the method / offset for speed: accuracy limitation of depth maps;  
high-resolution depthmaps (above  $512^2$ ) cost a lot of performance
- 165 • registration then has source- and target 2D-3D point pairs (in a normalized  
manner) that are put into a least-squares optimization system (give math  
here)
- optimization system usually non-linear, usually employing Levenberg-  
Marquardt optimization schemes [16]
- 170 • largest challenges for feature-based registration: (a) reliable feature cor-  
relation and (b) optimization stability; useful constraints can employed in  
both cases – such as horizon information, building edges, object outlines  
– to increase the registration reliability and accuracy
- employing constraints is highly application-dependent
- 175 • feature-based registration techniques most prevalent on mobile devices due  
to execution speed, implementation ease and so forth

- examples of mobile implementation: [17? , 18? ]; utilize open source library *OpenCV4Android*<sup>1</sup>, also employed in this work<sup>2</sup>
- drawback of feature-based methods: reliability and instability to imaging variances (discussed later in this article)
- a contrasting technique commonly achieving more accurate results: mutual information
- idea: pixel-wise comparison between 2D input image and 2D rendering of 3D scene; if both images match (meaning:  $\operatorname{argmin} \delta(I_{2D}, I'_{3D})$ ), then registration is completed
- mutual information [19] use notion of self-information and entropy to measure  $\delta(I_{2D}, I'_{3D})$
- challenge: optimization of 7 degree-of-freedom system over such over-determined system (i.e. each image pixel results in 2 equations for the optimization scheme) unstable and prone to local minima
- only optimization known to provide stable results is NEWUOA (i.e. Powell's method) [20];
- has recently been employed in an earth science case for lidar registration [? ]
- not available for mobile devices until now
- in terms of usability on mobile devices (why should we want to have that on mobile devices), projection of image-based information is vital on mobile devices
- because of interaction difficulty, image-based interpretations on 3D surface data is preferable

---

<sup>1</sup>OpenCV4Android - <https://opencv.org/platforms/android/>

<sup>2</sup>OpenCV4Android extensions at [https://github.com/CKehl/opencv4Android\\_extension](https://github.com/CKehl/opencv4Android_extension) and



- it is potentially advantageous, in terms of power consumption, to implement data interaction in 2D rather than 3D; a hypothesis proven by experiment in this article
- as it directly relates to the interactive component of the geoscience app, it has to be executed in real-time on the device instead of an offline process

205

#### 4.2. *Mesh-based rendering*

Rendering a surface model in this context refers to the image generation of the 3D data by projective rasterization to the 2D image plane of a virtual camera. This process is performed on mobile devices for the purpose of model presentation as well as for the generation of a synthetic reference image for image-to-geometry registration. Furthermore, it can be used to synthesize an image from available 3D data for interpretation and annotation in 2D.

Algorithms for rendering textured triangulated surfaces are well-known amongst technology-affine personnel. In the common rendering pipeline, the textured mesh is transferred as a set of (attributed) vertices and primitive sets (e.g. triangles, polygons) to the graphics processing unit (GPU). The virtual camera is set up using the pre-defined view projection matrix while the graphics primitives are repositioned using the model-related transformation matrix. The rasterizer projects the available 3D information into the camera plane and performs hidden-surface removal. The result is a discrete-space pixel representation. Modern programmable shaders allow in-time vertex decompression (see [21]) as well as texture decompression (see section ??). Available textures are mapped as images on the surface using the texture coordinate vertex attributes. The mesh-based rendering algorithms employed on desktop computers are analogous to mobile devices, whereas the technological details are posing the actual challenges.

220

225

#### 4.3. *A novel approach to mobile point-based rendering*

In comparison to mesh-based rendering, simple point projection seems to be a nice alternative saving computational resources and efforts for post-processing

concerning outlier removal due to falsely surface reconstruction (e.g. blobs due to critic point normals). Thus, we simply project object points onto image plane using perspective projection with assumption of distortion-free ideal camera with centred principle point. Thus, the camera matrix  $\mathbf{K}$  equals identity matrix  $\mathbf{I}$  and can be neglected in the following equations that generally base on notations given by Szeliski(2010). First, applying a six-parameter transformation transfers three-dimensional object points from world reference frame  $\vec{X}_W$  into a 3D camera system  $\vec{X}_c$  using

$$\vec{X}_c = \mathbf{R} \left( \vec{X}_W - \vec{X}_0 \right) \quad (4)$$

where  $\mathbf{R}$  is a  $3 \times 3$  orthonormal rotation matrix and  $\vec{X}_0$  the translation vector to camera's projection center. For simplicity, the usage of the planar Cartesian UTM system with  $x$  pointing to the east and  $y$  pointing to the north with respect to the prevalent zone number. For  $z$  component, the height over the Earth Gravitational Model 1996 (EGM96) is advisable to use. Counting for homogeneous coordinates, we can describe the relation between camera  $\vec{X}_c$  and image coordinates  $\tilde{x}$  involving their depth components.

$$\begin{pmatrix} \tilde{u} \\ \tilde{v} \\ c_c \end{pmatrix} = \begin{pmatrix} x_c \\ y_c \\ z_c \end{pmatrix} \quad (5)$$

For image plane we introduce camera constant  $c_c$  that defines the distance between camera's sensor and projection center in  $[mm]$  and is also known as focal length  $f$ . To separate camera sensor system and image system, we use the term  $c_c$  when talking about sensor  $[mm]$  and  $f$  for digital image coordinates  $[px]$ . For conversion,  $c_c$  must be divided by sensor's pixel pitch. For 3D to 2D projection, homogeneous coordinates must be divided by their depth components resulting in inhomogeneous coordinates.

$$\vec{X}_{Cam} = \begin{pmatrix} \frac{\tilde{u}}{c_c} \\ \frac{\tilde{v}}{c_c} \\ 1 \end{pmatrix} = \begin{pmatrix} \frac{x_c}{z_c} \\ \frac{y_c}{z_c} \\ 1 \end{pmatrix} \quad (6)$$

Thus, two-dimensional coordinates can be described with

$$\begin{pmatrix} \tilde{u} \\ \tilde{v} \end{pmatrix} = \begin{pmatrix} \frac{x_c}{z_c} \cdot c_c \\ \frac{y_c}{z_c} \cdot c_c \end{pmatrix} \quad (7)$$

For a final transformation of 2D sensor coordinates into image pixels, we must shift the origin to left upper corner and scale the coordinates that are still in global units by pixel's relation in meters per pixel  $p_s$ . Finally, we derive image coordinates  $(u, v)$  for an ideal camera using

$$\begin{pmatrix} u \\ v \end{pmatrix} = \frac{1}{p_s} \begin{pmatrix} \frac{x_c}{z_c} \cdot c_c - u_0 \\ \frac{y_c}{z_c} \cdot c_c - v_0 \end{pmatrix} \quad (8)$$

#### 4.3.1. Calculation of 3D bounding box of interest and image plane

Referring to the described use case of situation-based water level determination using a smartphone-camera based gauge (6.1), we need to define a region of interest regarding 3D point projection to render only user's field of view (figure 1). Thus, bounding box defining points to be projected must be calculated using camera position and orientation from fused smartphone sensors. Thereby it must be noted, that the heading is used for viewing direction only, tilt and roll are excluded. Because of uncertainties regarding exterior information (??), bounding box must be expanded to cover more object space than described by sensors as well as cameras field of view. Because of possible noise due to positioning, constants  $r$  and  $dh$  describe the domain of projection center's uncertainties parallel to image plane. For errors in depth, we define the correction  $c = \frac{r}{\tan(H)}$  for shifting the projection center along camera axis. The box is widened by the horizontal  $H$  and vertical  $V$  opening angles with a fixed depth  $d$ . In order to generate reference data for image-2-geometry intersection to annotate 3D data by mobile imagery, the lateral accuracy given by mobile positioning system as well as the prevalent camera characteristics solve for the mentioned parameters. For camera based gauging, we set  $d = 200[m]$ . Regarding 3D point projection, each potential point will be checked laying in the box. Therefore, additional tiling of the 3D data set is advisable. Using the defined

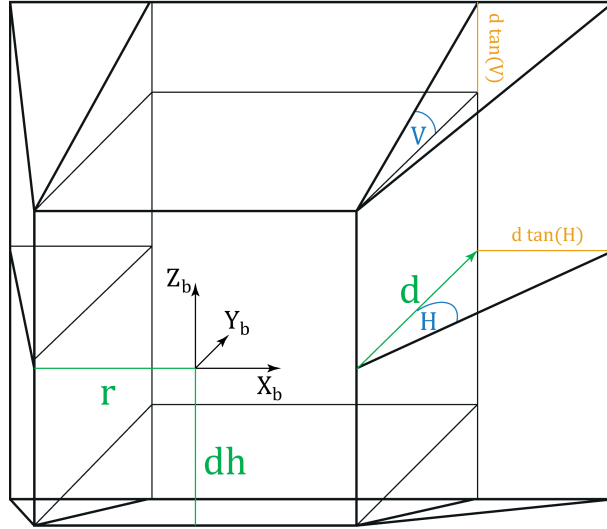


Figure 1: Bounding box definition.

frustum of a pyramid as region of interest with local reference system, the image plane for 3D point rendering can be defined by perspective projection of the remote  $xz$  plane (1) with

$$\vec{X}_b = \begin{pmatrix} -r - d \tan H \\ d \\ dh + d \tan V \end{pmatrix}$$

for bounding box' background plane upper left and

$$\vec{X}_b = \begin{pmatrix} r + d \tan H \\ d \\ -dh - d \tan V \end{pmatrix}$$

lower right corner. Its height equals the height component in world reference frame  $z_w$ . Because of pyramid frustum, we finally must eliminate outer points between the smaller front and larger rear plane considering the eight extremes.

workflow for outer point removal necessary?

230

#### 4.3.2. Pyramid approach for depth filtering

Because of a limited range of pixels with defined size inside a image plane  
 235 it seems to be obvious that in most cases more than one 3D object points  
 corresponds to the same image pixel. Due to inhomogeneous coordinates it is  
 not possible to figure out afterwards which points are in foreground compared  
 to the camera distances and which ones are behind and so not visible. This  
 problem can easily be solved during point cloud projection described above by  
 240 a simple camera-to-object distance check. However, one problem still remains  
 in case of e.g. glass fronts with lacking information (in TLS due to deflected  
 lidar or SfM when having homogeneous surfaces) or small archs (see figure ??)  
 Then, points might be visible pointing away from camera projection center. On  
 the one hand, point normals may solve the problem but due to data acquisition  
 245 technique and model's complexity, they are more or less easy to derive (Sattler  
 zitieren). Remedying image pyramids are a nice alternative approach used in  
 this case. Therefore, multiple synthetic images are generated with step-by-step  
 adjustment of  $p_s$  (see eq. 8), commonly by doubling which resulting in halve  
 numbers of image rows and columns per layer. Than, the algorithm verifies if  
 two pixels corresponds in two subsequent layers, preserving edges (figure 3, 2).

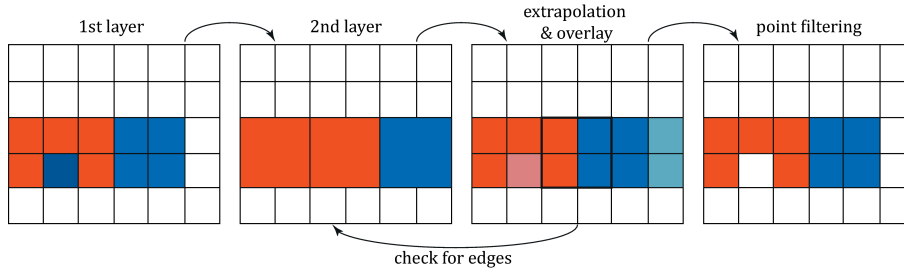


Figure 2: Visualisation of hierarchical depth filtering to handle point occlusions.

250

#### 4.3.3. Filling gaps due to missing points

**TO BE FILLED BY MELANIE**

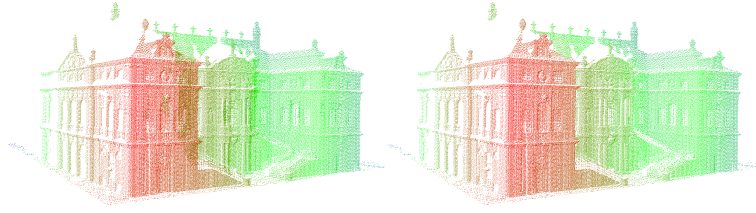


Figure 3: Left, actually obscured visible 3D points close to arches and windows. Right, edge preserving result after filtering.

#### 4.4. Interpretation and annotation

- short description what it does
- 255 • how is it generally employed
- relation to mobile devices
- approaches and implementation known on mobile devices
- integration to the above mentioned use cases
- Interpretation and annotation techniques (in this context used synonymously) aim to map geometries (e.g. lines, polygons) of domain-specific information to the 3D base surface
- 260 • the mapped geometries are used to delineate interest boundaries or segment the surface into semantically meaningful units
- in hydrological cases, line interpretations are commonly used to mark current water levels as well as high-tide or high-surge water levels
- 265 • for health monitoring of dykes and levees, line interpretations can also be used to mark cracks
- in geological cases, a mixture of line- and polygon geometries is used
- line interpretations are more commonly related to structural rock features (e.g. cracks, fractures, fault zone boundaries, stratigraphic boundaries),
- 270 • while polygonal area segmentation are more common in sedimentology

(e.g. depositional elements, sedimentary objects, sediment facies); application of the geometries is flexible, as in the case of fault facies for structural features

- 275 • delineation and mapping can be performed in various ways, depending on the geometric representation of the 3D surface geometry
- point clouds and 3D TINs can be annotated in 3D directly; area markings can be directly embedded as vertex attributes, whereas closest-vertex searches (for point clouds) or view-surface intersections (for TINs) provide  
280 the corners for line interpretations
- largest problem with such approach on mobile devices: data size and neighbourhood searches; nearest neighbour search has computational complexity  $O(nd)$  for  $d = 3$  (in case of 3D surfaces) and  $n$  being the number of vertices in the dataset; non-interactive on mobile devices with real-world  
285 datasets ( $n \geq 10^7$ )
- other issues: sparse and non-closed, non-convex geometry (particular problem for TINs), occlusions and curved objects; challenge specific to mobile devices: interaction, and the intuitive switch between 3D space motion and point selection
- 290 • using image-to-geometry registration, problems of 3D geometry and 3D space interaction can be circumvented
- image interpretation more computationally efficient due to raster arrangement (i.e. raster image) and easier to use for novice practitioners on mobile devices
- 295 • interpretation geometries rendered as 2D vector graphics elements and subsequently reprojected on 3D surface using the pre-determined external camera orientation (or pose)
- distinction between one-time interpretation and editing

- fixed interpretation markings can be trivially generated
- 300    – often approach is to delete the last marking (or manage an interaction history for further removals) and redraw incorrect interpretations
- for GRIT, more than 1,000 interpretation vertices need to be managed and edit requests are made by geologists; to facilitate a rapid edit and responsive interaction, a kD-Tree is maintained in the background to speed up interpretation vertex selection; kD-Tree is recalculated on significant point movements
- 305

## 5. Technology

### 5.1. Sensors

#### 5.1.1. Localization

- 310    • references: ...

#### 5.1.2. Orientation

- stability IMU (see 3D-NO)
- precision IMU

#### 5.1.3. Parameter sensitivity

### 315    5.2. Graphics

PUT SOMEWHERE HERE A REFERENCE TO osgAndroid AS EMPLOYED RENDERING LIBRARY

- as explained above, rendering 3D data is a key part for conducting annotations on 3D data, either based on 3D geometry itself or correlated images in camera space
- 320    • for mobile devices, this can technologically be realized two-fold, depending on the usage constraints



- 325

 • generally, rendering stages (image-plane projection, rasterization, tessellation & lighting, see [22]) can be realised by means of software or by hardware support
- 330

 • here, compute operations (gaussian smoothing, derivative computations, vertex projection) are implemented on the mobile device CPU by available operations and libraries using the Android SDK (Java) and Android NDK (C++) on Google's Android system and Swift and Objective-C on Apple's iOS platform
- 335

 • software-based rendering is more flexible in how operations are carried out as they do not need to account for hardware-specific processing pipelines; in the realm of mobile devices, non-standard software-based rendering operations are supported by a wider range of devices
- 340

 • drawback of software-based rendering is performance as it makes suboptimal use newer computing capabilities and graphics-specific chipset operations
- 345

 • example is the novel rendering approach for point-based rendering introduced in section ??, which requires implementation flexibility
- 350

 • most 3D rendering is done, even on mobile devices, with hardware-based rendering to varying degrees
- 355

 • even when implementing specific rasterization algorithms (see section ??), operations such as vertex projections and tessellation & lighting are performed on the GPU
- 360

 • hardware-based rendering on mobile devices is facilitated by Khronos' graphics library for embedded systems (GLES) [23] on specialised mobile device graphics chips (e.g. Qualcomm Adreno, ARM Mali, NVIDIA Tegra)
- 365

 • in comparison to software-based rendering, hardware acceleration provides improved performance

- drawbacks of hardware implementations are considerably longer development cycles, because the programming principles of GPUs differ considerably from common "App programming, and reduced flexibility on what can be realised
- 355 • for geoscientists and domain experts in the field, the distinction is good to be aware of as accelerated graphical apps for solving domain-specific tasks are usually offered as paid services to offset the increased development costs
- 360 • external circumstances and project constraints may govern implementation details for graphical systems
- major constraint imposed in this context is internet availability
- applications that are expected to operate in an urban setting or in well-developed infrastructure environments can make use of internet access
- 365 • this allows the externalisation of rendering tasks for 3D models and data to a network-oriented client-server architecture as in Ponchio et al. [21]
- field experts that use apps and require 3D-rendered information can submit rendering requests to a remote server that takes over the image generation of the 3D data
- 370 • technically, the app then only transmits metadata about storage location of the 3D data and receives the final, rasterised image, which allow energy-efficient operability
- 375 • furthermore, the process is agnostic to the specific mobile device generating the request, so this way of implementation works in the exact same manner for all mobile device regardless of the system manufacturer (e.g. Google, Apple, Microsoft)
- the reduced process load by externalising the rendering tasks allows using advanced algorithms for sensor tracking [] for improved localisation and

orientation or augmented reality [] for information overlays and multimedia content

- 380 • in other geoscientific settings, such as field geology [] and environmental monitoring [] of remote areas, internet access is either restricted or expensive to establish
- subscription to satellite network with the required data rate costs around 70 euro per month \$ (see [www.skydsl.eu](http://www.skydsl.eu), skyDSL2+ flatrate with 30 MBit/s download); data rate needed as high-resolution images with real-time rendering rates (uncompressed 1920x1080 pixels resolution at 30 frames/s amounts to 1.39 GBit/s) requires highest data rates even when employing advanced compression techniques
- 385 • thus, for geoscience applications that operate in remote areas, web-based rendering is not an option
- 390 • in these cases, rendering needs to be done on the device
- for on-device rendering, the 3D data need to reside in the device memory and image generation needs to be done with performance-restricted hardware
- 395 • as is shown in section ??, on-device rendering has considerable impact on the energy consumption
- on-device rendering that processes realistic field data requires considerable implementation efforts, as demonstrated by apps such as OpenWaterLevel [], GRIT [24] and Outcrop [25]
- 400 • principle scientific advances in mobile device rendering have demonstrated considerable progress over the years [13, 16, 26]
- scaling up smaller laboratory results with mobile graphics to realistic geoscience data, in terms of image quality and resolution as well as 3D base data, is a persisting challenge

- 405 • although technical development continuously provides more powerful devices, mobile devices need to sacrifice capabilities such as sensor availability as well as physical size and weight in order to provide larger memory space and higher-performance processors; examples for this trade-off manufacturing can be seen in special-purpose and high-performance tablets
- 410 such as NVIDIA Shield<sup>3</sup>, Project Tango resp. ARCore<sup>4</sup> and Google Pixel C<sup>5</sup>
- an specific problem for geoscientists and domain experts in on-device rendering settings: trade-off between app response time, image quality, hardware utilization and cross-device operability
- 415 • in interviews amongst field geologists at the department of earth science at university of Bergen, a major demand from the target user base of such mobile app is interoperability between Android, Microsoft and Apple devices; demand originates from platform-agnostic working of common geoscience software on desktop computers for Apple and Windows
- 420 • on the other hand, app responsiveness and high image quality are amongst the next common priorities behind interoperability; user base asks for improved quality when operating advanced equipment (e.g. special-pirpose tablets, novel- and high-performance tablets)
- 425 • both demands are conflicting, as making use of specialised hardware (e.g. 64-bit, streaming SIMD extensions (SSE) and vectorisation, parallel processing and GPU Computing such as CUDA<sup>6</sup> for image processing [27, 28], texture compression [29]) in turn means reducing the range of devices being able to operate the software
- these technologies are key as they provide technical solutions available

---

<sup>3</sup>NVIDIA Shield - <https://developer.nvidia.com/develop4shield>

<sup>4</sup>Google Augmented Reality - <https://developers.google.com/ar/>

<sup>5</sup>Google Pixel C- <https://www.android.com/tablets/pixel-c/>

<sup>6</sup>CUDA - <https://developer.nvidia.com/cuda-zone>

430 right now to achieve the required responsiveness and image quality

### 5.3. Power consumption

- power consumption is a metric of major importance for mobile field applications
- metric governs the operation time of an app outdoors for specific studies;  
435 in application domains such as field geology, the target operation time is in the range of four to eight hours without recharging at an electricity plug
- for the use cases of waterline detection and field interpretation, we measured the energy consumption of the apps "OpenWaterLevel" and "GRIT"  
440 and its relation to technical indicators, such as central processing unit (CPU)- and GPU utilisation, memory consumption and environment measures that influence chip operations, namely the processor temperature
- the following measures for both apps were obtained on a Google Nexus 5  
445 smartphone with 4-core ARM Cortex CPU and Qualcomm Adreno GPU; furthermore, OpenWaterLevels and its CPU-related measures were validated on a Samsung S8 smartphone with an 8-core ARM Cortex CPU of newer generation
- currently, the only app available on Android that allows measuring metrics  
450 on an app-specific level (i.e. logging the power consumption related to just one specific external app) is the Trepro Profiler <sup>7</sup>
- while this profiling app runs on all Android devices, the metrics that can be recorded (e.g. GPU load, processor temperature) vary between devices, so that GPU load measurements are not available for the Samsung S8  
455 smartphone

---

<sup>7</sup>Trepro Profiler -

- also the reason why measurements have been carried out on Google smart-phones instead of other tablets; general insight on processor-power consumption behaviour are possible to be extrapolated to other devices
- in the first test, we compare the power consumption in relation to CPU-  
460 and GPU utilisation
- our initial expectation is the a higher GPU load results in an increased power consumption compared to CPU-dominated operations, because mobile GPUs draw more power than CPUs to realise the increased graphics performance
- the results are shown for GRIT during 6.5 minutes of operations in fig. ?? (split in GPU and CPU contribution) and for OpenWaterLevel during  
465 3.5 minutes of operations in fig. ??
- observable in both apps: a clear dependency with CPU load and power consumption; shows that apps enter a state of conservative energy consumption if being inactive  
470
- furthermore, when comparing CPU-dependent and GPU-dependent energy graphs, we observe that peak energy consumption strongly relates to GPU activity
- for measurements in "GRIT", we also have to distinguish between two  
475 operation modes
- actions such as image-to-geometry registration [] and 3D outcrop viewing employ 3D data processing and GPU computations in a major scale, while the image-based interpretation of an outcrop uses 2D image operations within Android-optimized data structures
- fig. ?? and ?? depict the 2D use case, whereas fig. ?? and ?? show the  
480 energy consumption in 3D operations

- as clearly observable in fig. ?? in comparison to fig. ??, the 3D operations result in a drastic energy cost, raising the average power consumption by XYZ mA
- 485 • in contrast to novice expectation, the CPU load also increases in a 3D data processing setting
- that is because the CPU of the mobile processor needs to deliver the geometric- and texture data to the GPU; also, the CPU needs to decompress the texture image files, resulting in a higher processing load
- 490 • conclusions from the measurements are manifold
- on the level of assessing the profiled apps "OpenWaterLevel" for hydrological studies and "GRIT" for field geology studies, we obtained benchmark measures for their power consumption
- for OpenWaterLevels, the app can be operated with an average of XYZ mA per minute (XYZ mA/h), allowing a theoretical operability on a Google Nexus 5 smartphone of XYZ hours
- 495 • for GRIT, we distinguish between 2D- and 3D operability
- in 2D operation mode, only conducting image-based interpretations, GRIT consumes XYZ mA per minute (XYZ) per hours, allow XYZ hours of operation
- 500 • on the other hand, if being operated consistently in 3D-mode, the same app consumes XYZ mA per minute (XYZ) per hours, allow only 0.something hours of operation
- more generally speaking, the study shows that it is important for geoscience users to be aware of the which data they are working with
- 505 • on the mobile device
- even though 3D may be readily available for a given study, it is not advisable to access them on the mobile device over stretched periods, as the

drastically increased power consumption results in an operation time of  
510 XYZ hours with two external power packs in the field bag

- considering the CPU load behaviour in 3D-mode, we can also hypothesize about the positive impact of utilising hardware-specific operations such as GPU texture decompression on energy consumption: while using the GPU requires generally more power, it is also more efficient in operations such  
515 as texture decompression, therefore potentially having a positive affect on the overall power consumption of mobile field apps

## 6. Applications and Requirements

Due to the increasing usability of mobile devices for in the field annotations, several use cases concerning geosciences has become apparent. In the following,  
520 two essential

### 6.1. Derivation of hydrological parameters: Water level gauging

The last decade is characterized by a continued increase of globally devastating flash floods after heavy rainfalls. Even smallest creeks turned into hazardous streams causing flooding and landslides. Conventional gauging stations provide  
525 precise information about water levels measured over a short time period. State of the art techniques for administrative observation comprise water pressure sensors, floating gauges and conventional tide gauges. They are characterised by long-term stability and outdoor robustness providing accuracies of several millimeters up to one centimeter [30]. Averaged over defined time intervals, it is  
530 advisable to remain caution regarding these accuracies may be too optimistic [31] .

Because of high costs in purchase and maintenance, gauging stations with complex sensing devices must be sparsely installed. A prime example here is the hydrological network in Saxony, Germany. Here, 184 gauging stations  
535 are installed for permanent observation on 154 of 259 rivers rising from small, medium and large catchments [32, 33]. Thus, around a third is not monitored



neither during flood events when the most protection is required. Recently, commercial smartphone applications arose to enable crowd-sourcing based water level estimation for, among other things, such cases [34, 35]. But all of them have  
 540 one thing in common: the water level is entered manually by engaged citizen scientists finding and photographing tide gauges close to rivers that makes - on the one hand a potential danger to themselves (f.e. by sudden landslides), and still limits on the other the approaches to open and visible gauges.

Improvements in this sense can be achieved through *image-2-geometry intersection* and 3D annotation for automatic water level determination without  
 545 reference gauges for almost every situation regarding running waters. for this, the smartphone application *Open Water Level* that bases on the freely available open source camera framework *Open Camera* [36]. Open Water Level allows for free stationing water line detection using short hand held time-lapse image  
 550 sequences (for details please refer to [? ]). To interpret these, image measurements must be transformed into object space. Thus, exterior information needs to be provided by smartphone sensors for orientation and positioning.

#### 6.1.1.1. Requirements applying to the sensors

To solve the task of autonomous water level determination on running rivers  
 555 f.e. emergency cases using *image-2-geometry intersection*, citizen scientists position and orientation must be know. As figured out in 5, smartphone sensors accuracies for orientation and location are highly dependent on user's environment. Especially the strong correlation of heading and disturbing magnetic sources may be a issue must be solved specifically related to running rivers where  
 560 metal railings usually exists. Similar effects can also be noted using high-end IMU systems for instance autonomous car navigation. But the magnetic influences inside cars are almost stable and can be calibrated during the drive (advanced navigation manual). For smartphone orientation, the magnetic strengths attaching the phone may change substantially in short time. A typical scenario  
 565 would be: a citizen scientist walks along street, taking his phone inside the baggage close to metallic keys. While walking he passes several street lamps, signs,

etc. Finally, he arrives at a bridge over a urban river, takes out the phone, looks down to the river and records the time lapse image sequence a few centimetres above a metallic railing. Meanwhile, several cars passing the same bridge. In this simple use case, the magnetic field around the smartphone changes countless times due to several unpredictable disturbances (`table`mag`disturb`) [37]. The heading angle has the highest influence compared to pitch and roll regarding 2D image and 3D object data registration. For this, a so-called synthetic image is rendered from colored 3D reference point clouds using scientist's location and orientation to define a situation-dependent bounding box of points to be projected onto image plane with respect to depth and indentations (see [38]). Thereby the heading defines the rotation of the depth direction, as a false angle gives a false viewing direction resulting in a synthetic image that has no similarity or only a little with the time lapse sequence. However, in case of no similarity and thus no possible solution for *image-2-geometry intersection*, simply no water level can be calculated. But in case of slight overlapping, there might be image matches but with very bad distribution that impedes a correct positioning (`fig`heading`test`) and may lead to even worse results of false water levels.

It is obvious that a second source for destructive results exists: the absolute geo-positioning using smartphones currently installed GNSS receivers. In urban scenes with several shadow effects due to high-rise buildings, errors of several meters in latitude and up to more than 30 meters in height are highly possible where even the weather has impact [39, 37, 40]. It is likely that, in the near future, smartphone's GNSS modules will be improved solving lateral accuracies of 50 centimetres [41].

For now, possible relief might come including other sources for positioning like digital elevation models for simple height correction or invoke map services that allows the user for position refinement. For this, some APIs are already provided by Google (`quellen`) but they are rather cost-expensive by extensive accessing. Another upcoming option is including barometers in sensor fusion, altitude can be measured within three meters [42] but for now, they are not a standard.

- (table, observation heading during water line detection outside → check magnetic strengthens and there changes over short times)
- 600 • (figure/table, sensitivity analysis → heading changed in terms of 10 degrees, what does it make for)

### 6.1.2. Requirements applying to the scenario

- *online processing and position refinement: need online connection*
- 605 • *image quality for water line detection: influence of image resolution, lighting, ...)*
- available approach to address the task

## 6.2. Field Geology

The goal of geological fieldtrips is to gather insight in the rock record and the structural- and sedimentary rock architecture of a given location. Rock architecture can be studied within subsurface seismic records, but this approach 610 suffers from inferior imaging resolutions and physical limitations of the surveying technique. Therefore, surface outcrops are used for the study. Outcrops can be scanned with modern equipment (e.g. lidar [4, 43], drones [44] and SfM [45]) to generate digital surface representations. The most common representations of digital outcrops are coloured point clouds and textured TINs. 615

The geological aspect is introduced by interpreting the outcrop models. In this case, interpretations refer to (i) line marks for separating stratigraphic layers, (ii) surface-projected polygons to highlight structural- and sedimentary facies or specific architectural elements and (iii) minor ticks (e.g. lines, points, 620 patterns) to indicate depositional attributes such as deposition orientation or grain geometry. The interpretations was until recently performed in a two-step process: sketches are drawn by hand in the field to document the field geologist's observation of the architecture. After the fieldtrip, the observations are digitalised in the office by transferring the sketched architecture on the 625 available digital outcrop. From there on, further study goals (e.g. geomodelling)

are pursued. As recently published, this workflow is currently being transformed into an integrated digital workflow in the field using mobile devices (see [46] for further details).

Geological interpretations can be documented on various scales, but from ob-  
630 servations of the author most interpretations are conducted on medium-range. This results in an average observation distance for architectural interpretations of between 100m to 500m to document individual depositional elements and further distances of around 400m to 1400m to document the overall stratigraphic framework of an outcrop. Therefore, as a result of perspective observations,  
635 the required lateral localisation accuracy is in the range of  $\leq 2.5m$  for the individual element setting and  $\leq 8m$  for the wide-angle stratigraphic setting. While achieving the former resolution can still be challenging with mobile sensors (see section ??), the latter resolution is almost guaranteed for GPS localisation. The more important problem is in the vertical resolution: the vertical observation  
640 position has, especially in close-distance observations, a drastic impact on the view perspective. Even more important, a vertical localisation error of  $\geq 1.5m$  may result in positioning the mobile device "under ground", making any image-based registration impossible. It is this vertical accuracy that is crucial for mobile device interpretation systems to work. Several improvements, such as  
645 DEMs and barometric altitude [47], have been proposed to reduce the vertical positioning error while there is still room for novel research proposals to provide more accurate vertical positioning or ground-based constraints on the altitude estimation.

One of the dominant challenges for digital field geology is the free availabil-  
650 ity of 3D surface models. Currently, research groups in the domain (e.g. from the University of Manchester, Durham University, University of Aberdeen, University of Bergen and UniResearch CIPR) are building their own digital outcrop databases. Due to the strong industry involvement, these and other databases (see SAFARI [48] and FAKTS [49]) are excluded from public access. Recent de-  
655 velopments aim at providing digital outcrops in an open-access manner [50] to resolve the issue. Furthermore, due to the vertical positioning problem above,

easy access to high- and medium resolution DEMs is important. As demonstrated by recent measurement, the usage of DEMs has a significant influence on the projection accuracy of image-based interpretation on mobile device towards 3D surface models [47].

One particular challenge in digital field geology is the treatment of environmental changes. Digital outcrops are infrequently collected and the textured models are used for field study all across the year. Therefore, in image registration terms, there is a drastic difference in local illumination, moisture content as well as fog and snow between acquired 3D surface models and the outcrop images collected during field trips. The issue has been previously discussed in terms of illumination differences [18], but drastic changes in terms of fog and moisture are still problematic to treat. Therefore, it is advisable to collect digital outcrop models for prominent locations in different seasonal conditions to allow for variety in model selection when planning field trips.

Currently available systems that provide digital outcrop interpretation capabilities on mobile devices in 3D include GRIT [24] and Outcrop [25], though earlier prototypes have been demonstrated [51]. Outcrop, developed by Centre Européen de Recherche et d’Enseignement des Géosciences de l’Environnement (CEREGE) at Aix-Marseille Université, is a mobile device app for Android devices that is able to load and process various forms of numerical outcrops. Its major focus is the documentation of structural features (e.g. fault areas, fractures and rock deformations) on outcrops using line interpretations. Furthermore, it is possible to pin extended note annotations to the model. GRIT, developed as a collaboration between UniResearch AS CIPR, University of Bergen, University of Aberdeen and CEREGE, is a mobile device app for Android devices that can handle large-area digital outcrops of tens of kilometres in surface length in 3D. Its major focus is the documentation of the sedimentary- and stratigraphic architecture (e.g. strata boundaries, depositional object envelopes, facies areas) on outcrops via lines, polygons and brushes. The interpretations are mapped in a 2D-3D interplay between outcrop surface and field photograph.

[comparison photo: GRIT and Outcrop]

- recap: task to be solved
- main requirements for (location- and orientation) sensor accuracy and  
690 geometric accuracy
- specific requirements to this use case: data availability; illumination; network inavailability
- available approach to address the task

### 6.3. Virtual Field Trips

- recap: task to be solved
- main requirements for (location- and orientation) sensor accuracy and  
geometric accuracy
- specific requirements to this use case: data availability; illumination; network inavailability
- available approach to address the task

## 7. Conclusions

This article assessed the possibility of interactive interpretation and annotation of 3D outcrops on mobile devices in multiple geoscientific domains. Due to the research effort in recent years, novel mobile applications such as Open-  
705 WaterLevels for surface hydrology and GRIT for field geology were introduced to the community to bridge the gap between lab assessment and outdoor field work for data interpretation. This article also showed further application areas that build upon mobile device technology and the interactive annotation of 3D surface data for geoscientific problem solving.

710 McCaffery et al. proposed the use of mobile devices for field interpretation in geology in 2005 [3]. The technological specifics of mobile device app development hampered the progress on this goal for years. Only recent advancements in efficient treatment of 3D data [? ], algorithmic proposals for image-to-geometry

registration (see [17, 47]) and on-device 3D rendering (as presented in [26] and in  
 715 this article for point-based surface) specifically designed for mobile devices make  
 the actual use for geoscientific applications in the field possible. The utilisation  
 of crowdsourced VGI and introduction of mobile devices as low-cost measuring  
 devices for real-world problems [52] contribute to the acceptance of this mobile  
 device technological development within the geoscientific community. Computer  
 720 Vision challenges such as image registration under changing illumination condi-  
 tions and with reduced image resolution can be viewed as "sufficiently solved"  
 to make photogrammetric- and vision-based algorithms applicable to real-world  
 outdoor settings, while still leaving space for improvement and quality and per-  
 formance.

725 The measurements found in this article as well as its related studies suggest  
 that localisation and orientation of mobile device sensors with respect to the  
 application-specific accuracy requirements is a persisting challenge. The sensors  
 employed by low-cost devices have accuracy limitations. Sensor filtering- and fu-  
 sion techniques are required to even moderately consider the use of such sensor  
 730 data. Environmental effects such as device-internal heating processes and the  
 system-internal handling of sensor initialisation further complicate the calibra-  
 tion of such sensors without user involvement.

Furthermore, this study gives a representative overview about the energy  
 consumption of mobile apps employing 3D surfaces, computer vision and com-  
 735 puter graphics procedures. It was shown that the distinction between 2D- and  
 3D data used by mobile apps significantly drives the power consumption, and  
 therefore the operation time of the mobile field apps during a study. Means of  
 reducing the power consumption in the future have, next to extended periods  
 of app use by domain experts, beneficial secondary effects: power-reduced main  
 740 functions of the mobile app allow energy-expensive simultaneous localisation  
 and mapping (SLAM) techniques to be used for sensor data augmentation.

Lastly, the treatment of vegetation within scanned- and photographed data  
 during mobile field studies remains a challenge in the context of interactive in-  
 terpretation. 3D reference data are obtained less frequent than they are used

745 in a given outdoor setting. Vegetation itself is visually dynamic content that complicates image registration to existing 3D data, which complicates interpretations in common outdoor settings. While current procedures of data processing try to segment- and remove vegetation data from scans [], it leaves the mobile device app less information to work with when registering photos. Therefore, 750 proposing means of 3D topographic data processing that homogenizes vegetation in 3D scans and photos without removing the related data will have an impact on accurate outdoor photo registration on 3D base data.

## 8. Discussion

- porting existing desktop algorithms on mobile devices [quick and fast]
- 755 • pre-processing of geodata for mobile use

## Acknowledgements

Thank ESF, Richard Boerner for bounding box determination and image filtering

## References

- 760 [1] M. Kröhnert, C. Kehl, H. Litschke, S. J. Buckley, Image-to-geometry registration on mobile devices - concepts, challenges and applications, in: L. Paul, G. Stanke, M. Pochanke (Eds.), 3D-NordOst, volume 20, Gesellschaft zur Förderung angewandter Informatik, 2017, pp. 99–108.
- [2] I. Trinks, P. Clegg, K. McCaffrey, R. Jones, R. Hobbs, B. Holdsworth, 765 N. Holliman, J. Imber, S. Waggott, R. Wilson, Mapping and analysing virtual outcrops, Visual Geosciences 10 (2005) 13–19.
- [3] K. McCaffrey, R. Jones, R. Holdsworth, R. Wilson, P. Clegg, J. Imber, N. Holliman, I. Trinks, Unlocking the spatial dimension: digital technologies and the future of geoscience fieldwork, Journal of the Geological 770 Society 162 (2005) 927–938.



- [4] S. J. Buckley, J. A. Howell, H. D. Enge, T. H. Kurz, Terrestrial laser scanning in geology: data acquisition, processing and accuracy considerations, *Journal of the Geological Society* 165 (2008) 625–638.
- 775 [5] G. Caumon, G. Gray, C. Antoine, M. O. Titeux, Three-dimensional implicit stratigraphic model building from remote sensing data on tetrahedral meshes: Theory and application to a regional model of la popa basin, ne  
mexico, *IEEE Transactions on Geoscience and Remote Sensing* 51 (2013) 1613–1621.
- 780 [6] E. Schwalbe, H.-G. Maas, The determination of high-resolution spatiotemporal glacier motion fields from time-lapse sequences, *Earth Surface  
Dynamics* 5 (2017) 861–879.
- 785 [7] P. Letortu, M. Jaud, P. Grandjean, J. Ammann, S. Costa, O. Maquaire, R. Davidson, N. L. Dantec, C. Delacourt, Examining high-resolution survey methods for monitoring cliff erosion at an operational scale, *GIScience &  
Remote Sensing* (2017) 1–20.
- [8] M. Medjkane, O. Maquaire, S. Costa, T. Roulland, P. Letortu, C. Fauchard, R. Antoine, R. Davidson, High-resolution monitoring of complex coastal morphology changes: cross-efficiency of SfM and TLS-based survey (vaches-  
noires cliffs, normandy, france), *Landslides* (2018).
- 790 [9] Y. Watanabe, Y. Kawahara, UAV photogrammetry for monitoring changes in river topography and vegetation, *Procedia Engineering* 154 (2016) 317–325.
- 795 [10] M. Kröhnert, R. Meichsner, Segmentation of environmental time lapse image sequences for the determination of shore lines captured by handheld smartphone cameras, *ISPRS Annals of the Photogrammetry, Remote  
Sensing and Spatial Information Sciences IV-2/W4* (2017) 1–8.
- [11] J. G. Leskens, C. Kehl, T. Tutenel, T. Kol, G. de Haan, G. Stelling, E. Eise-  
mann, An interactive simulation and visualization tool for flood analysis

- usable for practitioners, *Mitigation and Adaptation Strategies for Global Change* (2015) 1–18.
- [12] E. N. Mueller, A. Pfister, Increasing occurrence of high-intensity rainstorm events relevant for the generation of soil erosion in a temperate lowland region in central europe, *Journal of Hydrology* 411 (2011) 266 – 278.
- [13] S. García, R. Pagés, D. Berjón, F. Morán, Textured splat-based point clouds for rendering in handheld devices, in: *Proceedings of the 20th International Conference on 3D Web Technology, Web3D '15*, ACM, New York, NY, USA, 2015, pp. 227–230. URL: <http://doi.acm.org/10.1145/2775292.2782779>.
- [14] T. G. Farr, P. A. Rosen, E. Caro, R. Crippen, R. Duren, S. Hensley, M. Kobrick, M. Paller, E. Rodriguez, L. Roth, et al., The shuttle radar topography mission, *Reviews of geophysics* 45 (2007).
- [15] C. Kehl, S. Buckley, R. Gawthorpe, I. Viola, J. Howell, DIRECT IMAGE-TO-GEOMETRY REGISTRATION USING MOBILE SENSOR DATA, *ISPRS Annals of Photogrammetry, Remote Sensing & Spatial Information Sciences* 3 (2016) 121–128.
- [16] C. Kehl, S. J. Buckley, J. A. Howell, Image-to-Geometry Registration on Mobile Devices - An Algorithmic Assessment, in: *Proceedings of the 3D-NordOst workshop*, volume 18, GFaI, 2015, pp. 17–26. ISBN 978-3-942709-14-9.
- [17] S. Gauglitz, C. Sweeney, J. Ventura, M. Turk, T. Hollerer, Model estimation and selection towards unconstrained real-time tracking and mapping, *Visualization and Computer Graphics, IEEE Transactions on* 20 (2014) 825–838.
- [18] C. Kehl, S. J. Buckley, S. Viseur, R. L. Gawthorpe, J. A. Howell, Automatic illumination-invariant image-to-geometry registration in outdoor environments, *The Photogrammetric Record* 32 (2017) 93–118.

- [19] P. Viola, W. M. Wells, Alignment by maximization of mutual information, *International journal of computer vision* 24 (1997) 137–154.
- [20] M. Corsini, M. Dellepiane, F. Ganovelli, R. Gherardi, A. Fusiello,  
830 R. Scopigno, Fully Automatic Registration of Image Sets on Approximate Geometry, *International journal of computer vision* 102 (2013) 91–111.
- [21] F. Ponchio, M. Dellepiane, Multiresolution and fast decompression for optimal web-based rendering, *Graphical Models* 88 (2016) 1 – 11.
- [22] J. Kessenich, G. Sellers, D. Shreiner, OpenGL Programming Guide: The  
835 Official Guide to Learning OpenGL, Version 4.5 with SPIR-V, OpenGL, Pearson Education, 2016. URL: <https://books.google.fr/books?id=vUK1DAAAQBAJ>.
- [23] P. Mehta, Learn OpenGL ES: For Mobile Game and Graphics Development, Apress, 2013. URL: <https://books.google.dk/books?id=Ra09AAAAQBAJ>.  
840
- [24] C. Kehl, J. R. Mullins, S. J. Buckley, R. L. Gawthorpe, J. A. Howell, I. Viola, S. Viseur, Geological Registration and Interpretation Toolbox (GRIT): A Visual and Interactive Approach for Geological Interpretation in the Field, in: *Proceedings of 2nd Virtual Geoscience Conference*, 2016, pp. 59–60.  
845
- [25] S. Viseur, R. Roudaut, R. Bertozzi, M. Castelli, J.-L. Mari, 3d interactive geological interpretations on digital outcrops using a touch pad, in: *Vertical Geology Conference (VGC)*, 2014.
- [26] M. Agus, E. Gobbetti, F. Marton, G. Pintore, P.-P. Vázquez, Mobile  
850 Graphics, in: A. Bousseau, D. Gutierrez (Eds.), *EuroGraphics 2017 - Tutorials*, The Eurographics Association, 2017. doi:10.2312/egt.20171032.
- [27] S. Heymann, K. Müller, A. Smolic, B. Froehlich, T. Wiegand, Sift implementation and optimization for general-purpose gpu, *Winter School of Computer Graphics (WSCG)* (2007).

- 855 [28] M. A. Hudelist, C. Cobârzan, K. Schoeffmann, Opencv performance measurements on mobile devices, in: Proceedings of International Conference on Multimedia Retrieval, ICMR '14, ACM, New York, NY, USA, 2014, pp. 479:479–479:482. URL: <http://doi.acm.org/10.1145/2578726.2578798>. doi:10.1145/2578726.2578798.
- 860 [29] D. Chait, Using ASTC Texture Compression for Game Assets, whitepaper, NVIDIA Corporation, 2015. URL: <https://developer.nvidia.com/astc-texture-compression-for-game-assets>.
- [30] S. Siedschlag, Wasserstände und Durchflüsse - messen, speichern und übertragen im digitalen Zeitalter, in: Dresdner Wasserbauliche Mitteilungen, volume 53 of *Dresdner Wasserbauliche Mitteilungen*, Technische Universität Dresden, Institut für Wasserbau und technische Hydromechanik, 2015. URL: <https://henry.baw.de/handle/20.500.11970/103357>.
- 865 [31] I. Horner, B. Renard, J. L. Coz, F. Branger, H. McMillan, G. Pierrefeu, Impact of stage measurement errors on streamflow uncertainty, Water Resources Research (2018).
- 870 [32] Saxon Flood Centre, Water levels & flow rates, 2018. URL: <https://www.umwelt.sachsen.de/umwelt/infosysteme/hwims/portal/web/wasserstand-uebersicht>, accessed: 2018-03-05.
- [33] U. Büttner, E. Wolf, Konzeption des gewässerkundlichen pegelnetzes in sachsen, 38. Dresdner Wasserbaukolloquium 2015 Messen und Überwachen im Wasserbau und am Gewässer (2015).
- 875 [34] S. Etter, B. Strobl, Crowdwater, 2018. URL: <http://www.crowdwater.ch/de/home/>, accessed: 2018-03-06.
- [35] Kisters, Einfach smart: App für Pegelmessung auf Knopfdruck, 2014. URL: [https://www.kisters.de/fileadmin/user\\_upload/Wasser/Produkte/WISKI/Produktblaetter/MobileWaterTracker\\_de\\_mail.pdf](https://www.kisters.de/fileadmin/user_upload/Wasser/Produkte/WISKI/Produktblaetter/MobileWaterTracker_de_mail.pdf), accessed: 2018-03-06.
- 880

- [36] M. Harman, Open Camera - Camera app for Android, 2017. URL: <https://sourceforge.net/projects/opencamera/>, version 1.38.
- 885 [37] J. R. Blum, D. G. Greencorn, J. R. Cooperstock, Smartphone sensor reliability for augmented reality applications, in: K. Zheng, M. Li, H. Jiang (Eds.), *Mobile and Ubiquitous Systems: Computing, Networking, and Services*, Springer Berlin Heidelberg, Berlin, Heidelberg, 2013, pp. 233 – 248.
- [38] R. Boerner, M. Kröhnert, Brute force matching between camera shots and synthetic images from point clouds, volume XLI-B5, 2016, pp. 771–777.  
890 doi:doi:10.5194/isprs-archives-XLI-B5-771-2016.
- [39] C. Bauer, On the (in-)accuracy of gps measures of smartphones: A study of running tracking applications, in: *Proceedings of International Conference on Advances in Mobile Computing & Multimedia, MoMM '13*, ACM, New York, NY, USA, 2013, pp. 335:335–335:341. URL: <http://doi.acm.org/10.1145/2536853.2536893>. doi:10.1145/2536853.2536893.  
895
- [40] P. A. Zandbergen, S. J. Barbeau, Positional accuracy of assisted GPS data from high-sensitivity GPS-enabled mobile phones, *Journal of Navigation* 64 (2011) 381–399.
- 900 [41] S. K. Moore, Superaccurate gps coming to smartphones in 2018, *IEEE Spectrum* (2017). Accessed: 2018-03-06.
- [42] G. Liu, K. M. A. Hossain, M. Iwai, M. Ito, Y. Tobe, K. Sezaki, D. Matekenya, Beyond horizontal location context: measuring elevation using smartphone’s barometer, in: *Proceedings of the 2014 ACM International Joint Conference on Pervasive and Ubiquitous Computing Adjunct Publication*, ACM Press, 2014. doi:10.1145/2638728.2641670.  
905
- [43] S. J. Buckley, E. Schwarz, V. Terlaky, J. A. Howell, R. Arnott, Combining Aerial Photogrammetry and Terrestrial Lidar for Reservoir Analog Modeling, *Photogrammetric Engineering & Remote Sensing* 76 (2010) 953–963.

- 910 [44] T. J. Dewez, J. Leroux, S. Morelli, Uav sensing of coastal cliff topography for rock fall hazard applications, in: Journées Aléas Gravitaires JAG 2015, 2015.
- [45] J. Chandler, S. Buckley, Structure from motion (SFM) photogrammetry vs terrestrial laser scanning, American Geosciences Institute (AGS), 2016.
- 915 [46] C. Kehl, J. R. Mullins, S. J. Buckley, J. A. Howell, R. L. Gawthorpe, Interpretation and mapping of geological features using mobile devices in outcrop geology - a case study of the saltwick formation, north yorkshire, uk, AGU Books - Special Issue (2018 (accepted for publication)).
- [47] C. Kehl, S. J. Buckley, S. Viseur, R. L. Gawthorpe, J. R. Mullins, J. A. Howell, Mapping field photos to textured surface meshes directly on mobile  
920 devices, The Photogrammetric Record 32 (2017) 398–423.
- [48] T. Dreyer, L.-M. Fält, T. Høy, R. Knarud, J.-L. Cuevas, et al., Sedimentary architecture of field analogues for reservoir information (SAFARI): a case study of the fluvial escanilla formation, spanish pyrenees, in: The  
925 Geological Modeling of Hydrocarbon Reservoirs and Outcrop Analogs, volume 15, International Association of Sedimentologists – Special Publications, Wiley Online Library, 1993, pp. 57–80.
- [49] L. Colombera, F. Felletti, N. P. Mountney, W. D. McCaffrey, A database approach for constraining stochastic simulations of the sedimentary  
930 heterogeneity of fluvial reservoirs, AAPG bulletin 96 (2012) 2143–2166.
- [50] A. J. Cawood, C. E. Bond, erock: an online, open-access repository of virtual outcrops and geological samples in 3d, in: EGU Geophysical Research Abstracts, volume 20, 2018, p. 18248.
- [51] L. Hama, R. A. Ruddle, D. Paton, 3d mobile visualization techniques in  
935 field geology interpretation: Evaluation of modern tablet applications, in: AAPG Hedberg Research Conference: 3D Structural Geologic Interpretation: Earth, Mind and Machine, 2013.

- [52] A. Eltner, H. Sardemann, M. Kröhnert, E. Schwalbe, Camera based low-cost system to monitor hydrological parameters in small catchments, in: EGU General Assembly Conference Abstracts, volume 19, 2017, p. 6698.

### Highlights

- point 1
- point 2
- point 3
- point 4
- point 5